PROCEEDINGS OF SPIE

Machine learning and hybrid metrology using scatterometry and LE-XRF to detect voids in copper lines

Dexin Kong, Koichi Motoyama, Abraham Arceo de la peña, Huai Huang, Brock Mendoza, et al.

SPIE.

Machine learning and hybrid metrology using scatterometry and LE-XRF to detect voids in copper lines

Dexin Kong [a], Koichi Motoyama [a], Abraham Arceo de la peña [a], Huai Huang [a], Brock Mendoza[a],
Mary Breton [a], Gangadhara Raja Muthinti [a], Hosadurga Shobha [a], Liying Jiang [a], Juntao Li [a], James
J. Demarest [a], John Gaudiello [a], Gauri Karve [a], Aron J. Cepler [b], Matthew Sendelbach [b], Susan
Emans [b], Paul Isbester [b], Kavita Shah [b], Shay Wolfling [c], Avron Ger [c]
[a] IBM, 257 Fuller Road, Albany, NY, 12203
[b] Nova Measuring Instruments, Inc., 3342 Gateway Blvd, Fremont CA 94538 USA
[c] Nova Measuring Instruments, LTD, P.O. Box 266, Weizmann Science Park, Rehovot 76100, Israel

ABSTRACT

Voids in copper lines are a common failure mechanism in the back end of line (BEOL) of integrated circuits manufacturing, affecting chip yield and reliability. As subsequent process nodes continue to shrink metal line dimensions, monitoring and control of these voids gain more and more importance [1]. Currently, there is no quantitative in-line metrology technique that allows voids to be identified and measured. This work aims to develop a new method to do so, by combining scatterometry (also referred to as Optical Critical Dimension or Optical CD) and low-energy x-ray fluorescence (LE-XRF), as well as machine learning techniques. By combining the inputs from these tools in the form of hybrid metrology, as well as with the incorporation of machine learning methods, we create a new metric, referred to as V_{xo}, to characterize the quantity of void. Additionally, the results are compared with in-line electrical test data, as higher amounts of voids were expected to increase the measured resistivity. This was not found to be the case, as the impact of the voids was much less of a factor than variation in the cross-sectional area of the lines.

Keywords: Scatterometry, machine learning, XRF, hybridized metrology, BEOL, voids

1. INTRODUCTION

A key source of yield loss in semiconductor manufacturing are voids, which are commonly found in the back-end-of-line (BEOL) copper lines. These voids are not able to be measured quantitatively or with in-line metrology; instead, destructive techniques such as TEM are used to look for voids after the process is completed. CD-SEMs could be used to detect voids on the exposed copper line but it is not used in manufacturing due to yield and reliability concern of a prolonged queue time before capping and difficulty in observation due to electrical charging. Given that the pitch of BEOL structures is continuing to decrease at each ensuing technology node, monitoring and control of these voids gain more and more importance [1-5] in order to maximize yield, performance, and reliability.

The goal of this work is to develop a new method to measure the amount of void inline, by combining scatterometry (also referred to as Optical Critical Dimension or Optical CD) and low-energy x-ray fluorescence (LE-XRF), as well as machine learning techniques. Optical CD is an inline metrology technique that is commonly used to measure structural dimensions, while XRF can obtain elemental

compositions. By combining the inputs from these tools using hybrid metrology, we create a new metric, referred to as V_{xo}, which combines inputs from Optical CD and XRF to characterize the amount of void.

A design-of-experiment (DOE) is set up to induce variation in the amount of voids in the copper line, with the samples having differing amounts of additional voids, above the normal expected voids from the process of record (POR). Voids are intentionally generated based on two methods: Overly thin copper seed layer, which can inhibit copper growth during the electrochemical plating (ECP) process, result in sidewall voids; and overly thick liner materials, which can cause pinch-off during the copper fill, leading to center voids. Those processes were illustrated in Figure 1 and Figure 2 below.
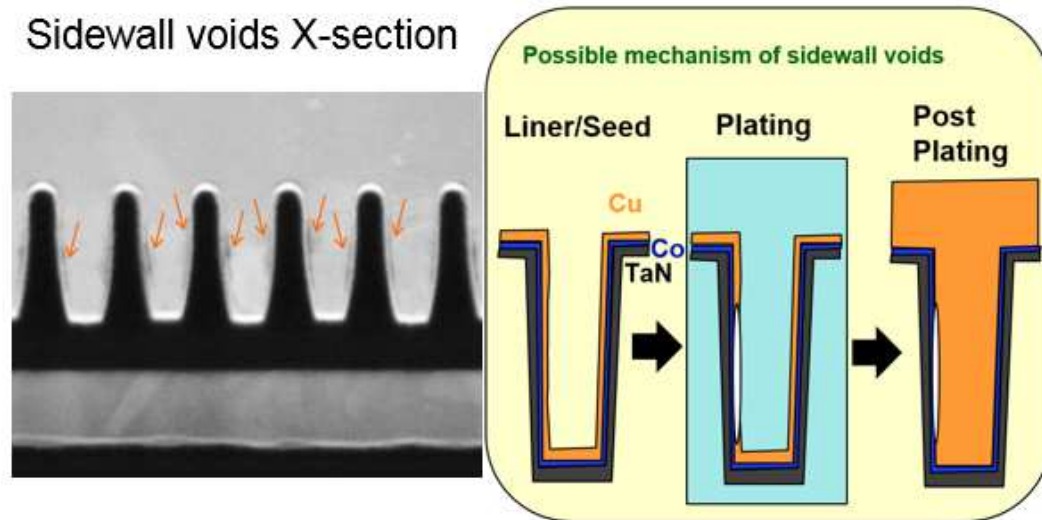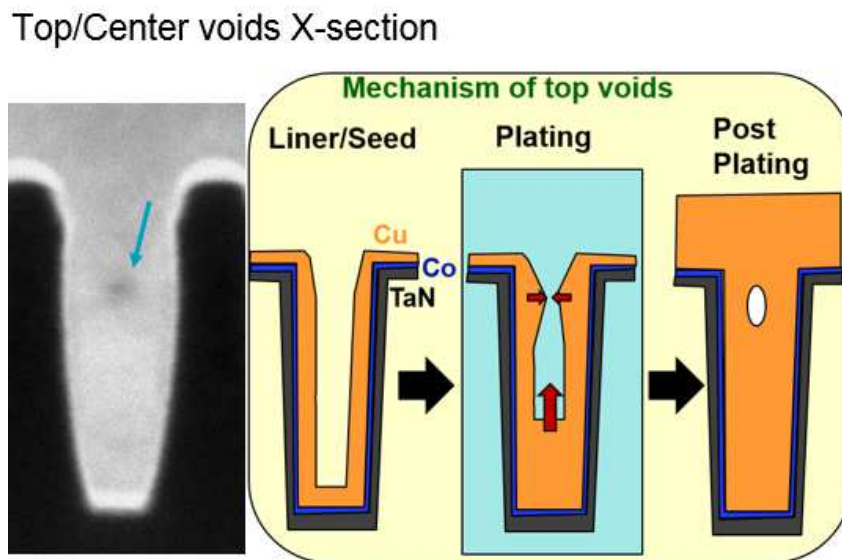

Figure 1: Possible mechanism of sidewall voids

Figure 2: Possible mechanism of top voids

2. EXPERIMENTAL METHODS

2.1 Scatterometry

Scatterometry is a ubiquitous 'workhorse' metrology tool, used for fast and non-destructive measurement of geometrical and material parameters [6-9]. Figure 3 shows a schematic explaining the operation of scatterometry tools. The wafers are measured in the scatterometry unit for raw spectra collection. A scatterometry model is required to interpret the raw spectra. The dimensional and material information can be retrieved by fitting spectra with the model. The model needs to be well calibrated with the transmission electron microscope (TEM) imaging, or other reference sources, for accurate measurement before installing the model on the tool. Once the model is calibrated and installed, the scatterometry measurement for the specific step can be activated for in-line measurement with high throughput. When working with scatterometry, the user must account for the time needed to build a model and the required resources for data calibration, e.g. TEM, CDSEM. Additionally, in the case of a significant process change or material change, the scatterometry model needs to be rebuilt with additional calibration resources and model rebuilding time.
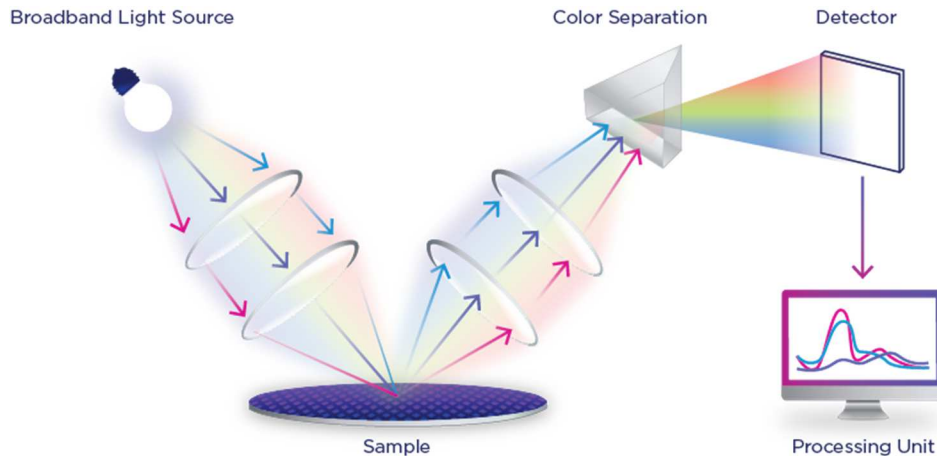

Figure 3: Schematic of optical scatterometry measurements.

2.2 LE-XRF

Low energy x-ray fluorescence (LE-XRF) is an inline metrology technique used primarily for material characterization [8], described in Figure 4 below. X-rays impinge on the sample, and the incident energy raises electrons to an excited state before falling back to their ground state. The amount of energy released as the electrons return to their ground state is characteristic to the specific element, and by monitoring the amount of each specific energy in the detection range, we can "count" the amount of each element in the sample.
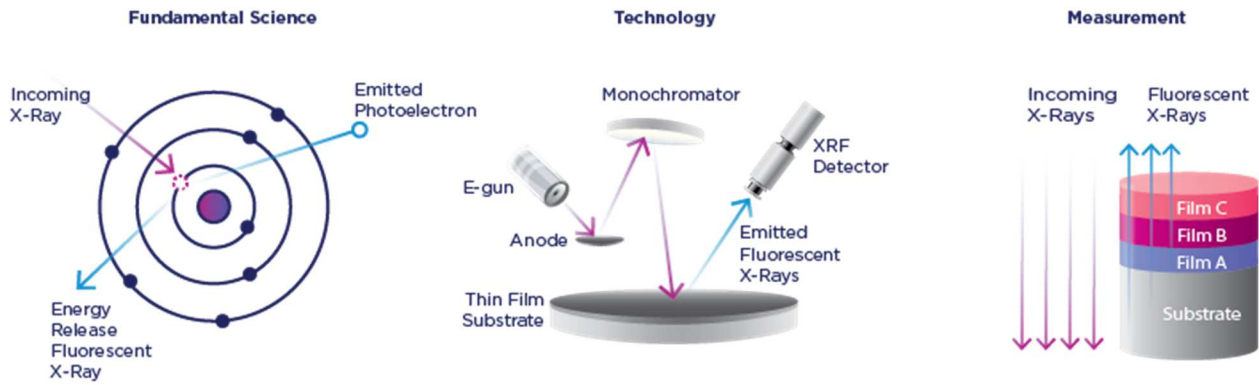
Figure 4: Schematic of low energy x-ray fluorescence measurements

2.3 TCR based resistivity measurement

Temperature coefficient of resistivity (TCR) [3, 10]based resistivity measurement is an offline electrical test, and it is widely used to characterize resistivity of metal lines in BEOL. The line resistance is measured at different temperatures, usually in the range between room temperature and 150C°. As described by Matthiessen's rule, the total resistivity is constituted by phonon scattering (bulk resistivity), impurity scattering, surface scattering, and grain boundary scattering. Only the bulk resistivity is considered as temperature dependent, and its temperature gradient ($d\rho$ /dT) is constant, also known as TCR. As a material property, TCR can be measured from bulk material or obtained from a reference. The copper cross-sectional area can be obtained from equation 1 and the total resistivity can be thereby calculated by equation 2.

$$A = L \frac{\left(\frac{d\rho}{dT}\right)}{\left(\frac{dR}{dT}\right)} \qquad \text{Eq. 1}$$

$$\rho = \frac{R*A}{L} \qquad \text{Eq. 2}$$

In both equations, A is the cross-sectional area of the copper line, L is line length, ρ is total resistivity, R is the messured line resistance, and T is temperature. TCR based resisitivity measurement is non-destructive and provides better differentiation (>2%) between experimental splits than the conventional TEM based resistivity measurement (>10%). In addition, the contribution of liner and barrier to the overall resistivity is typically not considered since their conduction is significantly lower than copper.

2.4 Machine Learning

Machine learning [9] is used in this work to enhance the throughput of the various techniques. Due to tool-time availability limitations, the sampling with LE-XRF and TCR was not as high as the sampling for Optical CD (which measured every die on every wafer). LE-XRF measured approximately 1/3 of the available dies on every wafer, and TCR measured every die on half of the available wafers. Machine learning allows the user to take the measured data from LE-XRF and TCR

and directly associate the data points with the Optical CD spectra. In this way, we can build a machine learning dataset which effectively extrapolates results from LE-XRF and TCR on to all die where Optical CD spectra are available. This procedure is shown schematically in **Error! Reference source not found.Error! Reference source not found.** and **Error! Reference source not found.Error! Reference source not found.**.
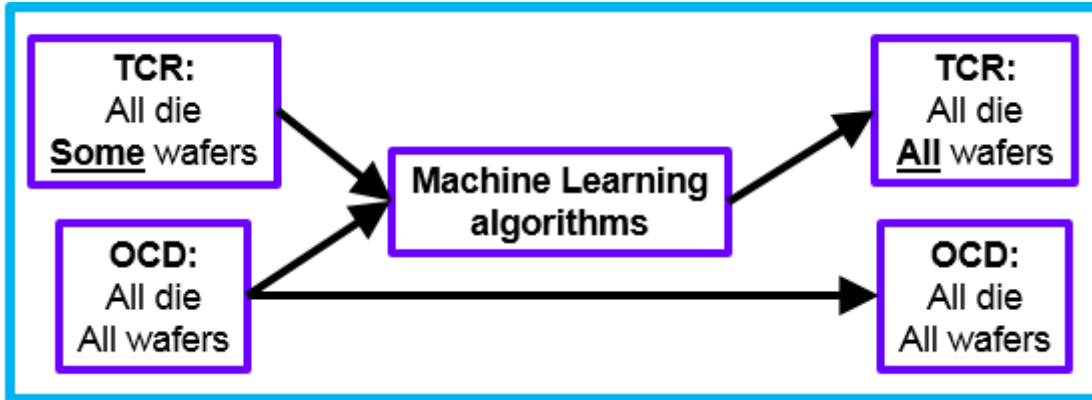

Figure 5: Illustration of machine learning algorithms used to apply TCR results from some wafers to all wafers
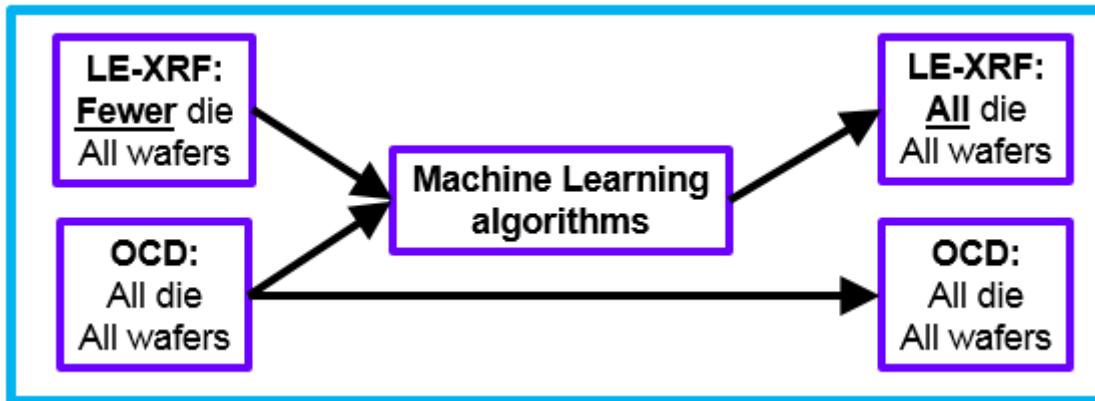

Figure 6: Illustration of machine learning algorithms to apply LE-XRF results from some die to all die

3. RESULTS AND ANALYSIS

As described in the introduction, voids in copper metal lines degrade device yield and BEOL reliability performance, so developing in-line metrologies is necessary to improve semiconductor device yield and reliability, especially for advanced 7nm node and beyond technologies. In this work, two in-line metrics are investigated for measuring voids, Cu resistivity and V_{xo} (derived parameter by hybridizing scatterometry and LE-XRF). The results are discussed in this section. The typical cross-sectional structure of prepared wafers is discussed in sub-section 3.1, followed by the discussion about in-line metrology data in next sub-section. In sub-section 3.3 and 3.4, we present the metric of resistivity and $V_{xo,}$ respectively. In sub-section 3.5, we discuss the value added by the use of machine learning algorithms.

3.1 Design of experiments

Copper lines in modern semiconductor technology BEOL structures are typically formed by first

depositing a copper seed layer by physical vapor deposition (PVD), then electrochemical plating which fills the rest of the trench with copper.

Based on the knowledge of the metallization process, changing the copper seed layer thickness can affect the quality of copper lines. The split conditions for the DOE are shown in Table 1 below. The first two wafers used reflow process, which is a well-established technique intended to reduce the presence of voids by annealing the wafers after the copper seed layer deposition [2-4]. The remaining wafers did not use the reflow process; instead, they were subjected to different seed layer thicknesses to study their effect on voids.

Table 1. The split conditions are listed in this table with 2 wafers per split. The seed layer thickness is normalized.

Wafer ID	Cu seed layer thickness (Normalized)
1	0.75 Cu reflow process
2	0.75 Cu reflow process
3	0.35
4	0.35
5	0.5
6	0.5
7	0.75
8	0.75
9	1
10	1

Figure 7 shows the cross-sectional structure of the copper metal lines from one of the prepared wafers. Based on the process assumption, the schematics of the structure are shown in Figure 7(a). The trench is formed by patterning and reactive ion-assisted etching of a dielectric substrate and followed by the sequential deposition of TaN barrier and cobalt liner. The copper seed layer is deposited with PVD, and electroplating is used to fill up the trench. Finally, chemical mechanical planarization (CMP) is used to remove the overfill and set the line height, and then the copper line is capped with cobalt and
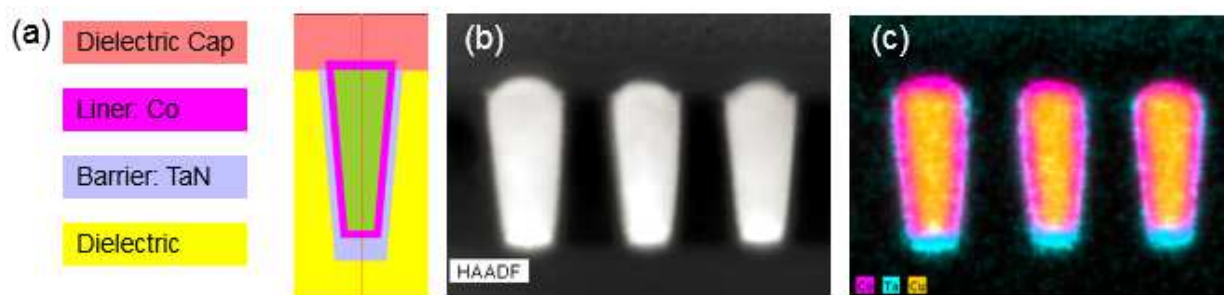

Figure 7 shows the cross-sectional structure of Cu metal lines. (a) shows the schematics of the structure. (b) shows the high-angle annular dark-field TEM image, from which metal and dielectric are clearly distinguished. (c) shows the elemental mapping image from EDX-TEM measurement, where the TaN barrier, Co liner and Cu are clearly resolved.

dielectric materials to avoid oxidization. Figure 7(b) shows the dark-field TEM image, which the metal

(bright region) is clearly distinguished from dielectric (dark) since the transmitted electron signal is sensitive to atomic number Z, $I \propto Z^4$. However, the barrier, liner, and Cu cannot be resolved for Figure 7(b). The elemental mapping was done with EDX-TEM scanning, as shown in Figure 7(c), where the TaN barrier, cobalt liner, and copper are clearly resolved in Figure 7(c).

3.2 Scatterometry and LE-XRF results

In this section, we discuss the data collected from in-line metrologies, scatterometry and LE-XRF. Scatterometry data was measured with NovaT600 and NovaMARS, and LE-XRF was collected with NovaVeraFlex IIIXF. Figure (a) shows the XRF measurement of all wafers, and it is a direct measurement of cobalt atoms in the illuminated area. Figure (b) contains the thickness measurement results from conventional scatterometry measurements, which is model-based metrology. These two completely different techniques show the same trend that the cobalt liner thickness varies along with the different split conditions.
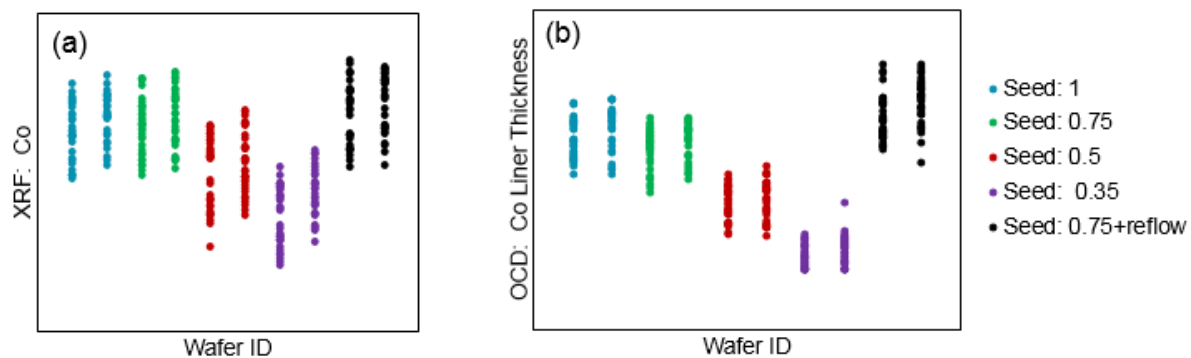

Figure 8. (a) shows the plot of XRF measurements of Co liner, and (b) shows the scatterometry measurement of Co liner with conventional modeling. XRF shows the same trend as OCD measurement for Co liner.

By experimental design, only the copper seed layer thickness varied for different split conditions, but not the cobalt liner. However, both XRF and scatterometry indicates that cobalt liner thickness changes with split conditions, which is an interesting result. The explanation for this observation is that the copper plating chemistry also erodes the cobalt when the copper seed layer is thinner than a threshold thickness. The plot of cobalt liner thickness is plotted against Cu seed layer thickness, as shown in Figure , where normalized cobalt liner thickness is in the *y*-axis and normalized copper seed layer is in the *x*-axis. From Figure , we see that the cobalt liner thickness decreases with the reduction of copper seed thickness when the copper seed thickness is below the threshold of 0.8. While the copper seed is above the threshold value, the cobalt liner thickness does not change with the thickness of the copper seed layer. Since Cu reflow process [4] can fill minimum trenches with Cu completely, Co liner is fully protected by Cu during the plating process. Therefore, the Co liner is thickest for Cu reflow split, as shown in fig. 9.

Both LE-XRF and scatterometry show the same result that cobalt liner thickness changes with the different split conditions as the copper seed layer thickness varies. As a consequence, the effective cross-section area of copper line is also changing with experimenting conditions. The electrical

properties of copper lines would also change when the cross-section area changes, which will be discussed in the next sub-section.
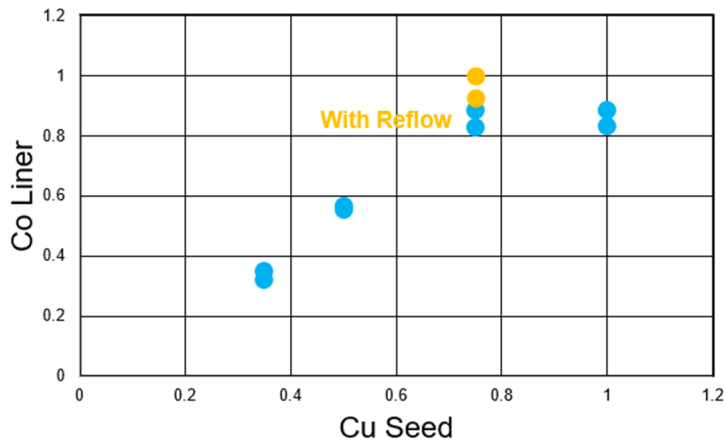

Figure 9 *show the plot of Co liner thickness (normalized) vs Cu seed layer thickness (normalized).*

3.3 Resistivity of Cu lines

The resistivity of copper metal lines was obtained via the Temperature Coefficient of Resistivity (TCR) based measurements described in the previous section. In Figure, the resistivity on the y-axis was plotted against the cross-sectional area of copper line on the x-axis. The cross-sectional area was obtained from scatterometry measurement with conventional modeling. Data points were collected from all wafers in the DOE, and the solid line is the empirical formula developed from advanced BEOL semiconductor technology [10]. The figure shows that resistivity decreases with the increase of metal line area, and the trend follows with the solid blue line of the empirical formula. In the
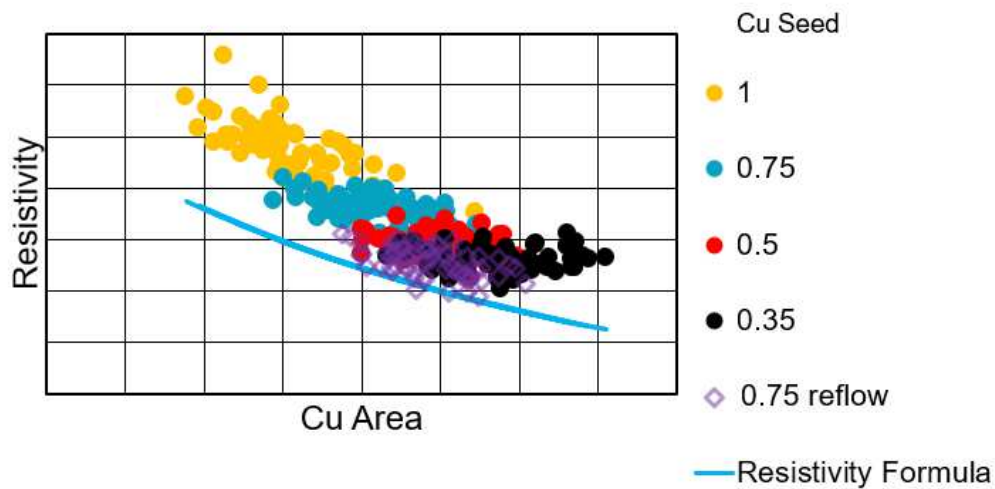

Figure 10: Resistivity, measured from temperature coefficient resistivity (TCR), versus the cross section area of Cu lines. It shows the Cu line resistivity decreases with the increase of Cu cross section area, and the trend follows the empirical formula.

nanometer scale, the resistivity of the copper line also depends on the size or area of metal lines due to the surface scattering of electrons.

In Figure, we see that the cross-sectional area of metal lines changes with split conditions. Specifically, the Cu line area increases as the normalized copper seed layer thickness changes from 1 to 0.35. As mentioned in section 3.2, the total trench area is the same, thinner liner left more room to Copper, plating erosion enhanded this effect. Figure also shows that the copper lines with the reflow process have lower resistivity than the ones without reflow at the same normalized copper seed layer thickness of 0.75.

Figure plots the resistivity as a function of our void metric, V_{xo}, which is derived from the hybridization of XRF and scatterometry. It shows that the resistivity for each split weakly correlates to V_{xo}, indicating that resistivity may not be a good measurement of the voids in this work.
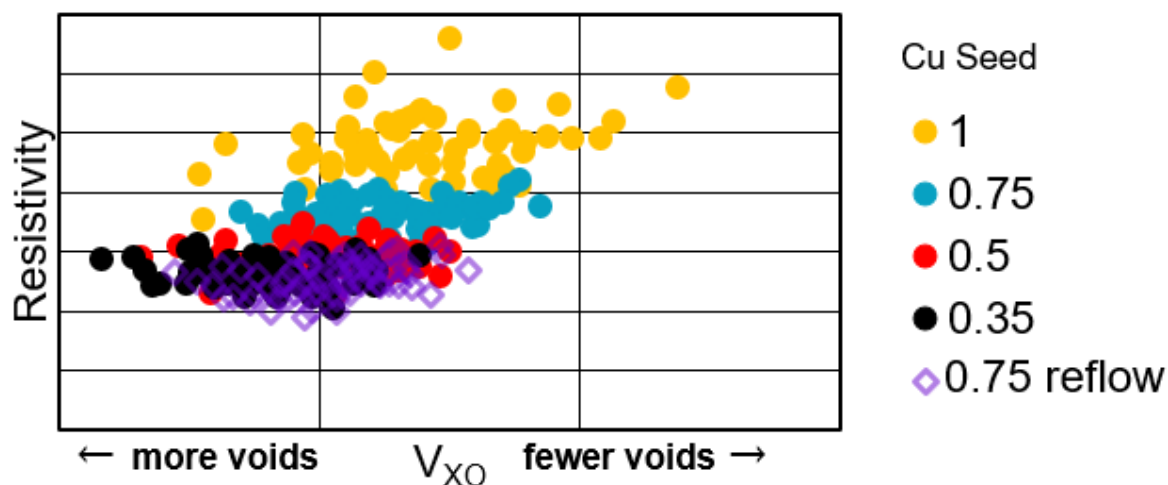

Figure 11: This plots resistivity as a function of the alternative metric, V_{xo}. The metric V_{xo} was a parameter developed from hybridizing scatterometry and LE-XRF.

Intuitively speaking, we should expect higher resistivity with more voids in metal lines. From the discussion in section 3.1, there should be more voids as copper seed layer thickness decreases, so we should expect higher resistivity for thinner copper seed layer split if the initial assumption is correct. However, the results shown in Figure does not agree with this speculation. It was discussed that the line resistivity depends on the microstructure of copper, voids and also the cross-sectional area when the critical dimension is in nanoscale. Figure clearly shows that resistivity increases as the copper cross section area decreases. Both voids and cross-sectional area are competing to affect line resistivity, but it seems that the cross-section area dominates the effect, at least, in the investigation range of experiment variations. The effect of voids to resistivity is over-shadowed by the cross-section area of copper lines.

This leads us to the conclusion that resistivity is not likely to be a good measurement of voids in copper metal lines. The other metric of V_{xo} will be evaluated in the next section.

3.4 The metric of V_{xo} from hybrid metrology

As mentioned previously, V_{xo} is a parameter obtained by hybridizing XRF with scatterometry techniques in a novel method. Higher V_{xo} indicates fewer voids in copper lines and vice versa. Figure plots the metric of V_{xo} on the y-axis as a function of copper seed layer thickness on the *x*-axis in terms of wafer average. The blue data points are from non-reflow splits, while the yellow data point is from the split condition with reflow. It is shown in Figure that blue data points strongly depend on the variation of copper seed thickness, and that is V_{xo} decreases (indicating more voids) as the copper seed layer is thinning down. Based on the processing knowledge, we should expect more voids as copper seed layer thickness decreases. Therefore, the relationship between V_{xo} and copper seed layer thickness, shown in Figure , matches the expectation from the originally designed experiment and splits.

The yellow data from reflow split falls off the trend shown in blue data points. Comparing it with the other blue data points without reflow, we can see that the amount of voids for Cu reflow splits is within the scattering range of no-reflow splits, but not obviously lower than no-reflow splits. This observation does not agree with our initial expectation since the majority opinion in the field believes reflow produce better quality copper lines. The reflow process generates Cu lines with V_{xo} parameter that is comparable with those without reflow. We do observe that the reflow process improves the resistivity of copper lines in Figure. This can be explained in that the reflow process improves the microstructure in copper lines, e.g. larger grain size and fewer grain boundaries, which reduces resistivity even the
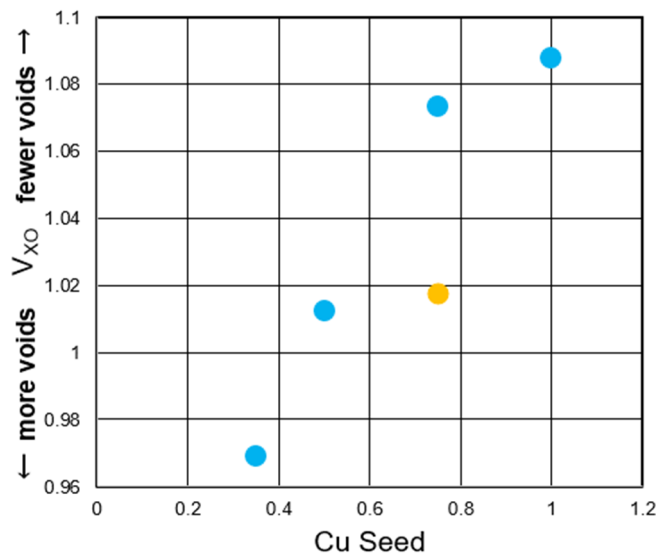

Figure 12: *The metric of V_{xo} is plotted against Cu seed layer thickness. The blue datapoints are wafer averages for no reflow splits, and the yellow datapoint is that with reflow split. Blue datapoints shows a strong correlation between V_{xo} and Cu seed thickness. This relationship matches the expectation from process knowledge.*

reflow split has comparable Vxo with no-reflow process. The effect of microstructure on electrical properties competes with voids, and microstructure has stronger effect than voids. Further investigation is needed to fully understand this observation.

Even though the relationship shown by blue data points in Figure matches the expectation, based on the process knowledge, it is not a strong indicator. Therefore, we can evaluate the metric of V_{xo} with respect to electromigration (EM) lifetime.

As discussed in section 3.2, the cobalt liner thickness also changes between splits, even though the copper seed layer is the only parameter we intentionally vary in the design of experiments. Figure is a plot of V_{xo} as a function of cobalt liner thickness, from which we can see the thinner cobalt liner thickness produces lower V_{xo} and more voids. In Figure , the EM lifetime is also plotted against cobalt liner thickness. EM lifetime is defined here by the time for 50% devices across a wafer to fail. Both Co/Cu interface quality (smoothness and uniformity) and voids in copper lines affect EM lifetime in the same manner. When all other processes are consistent but the cobalt liner thickness varies, which results in an assumption that the Co/Cu interface is similar, EM lifetime is a known indicator of the amounts of voids [10]. Shorter EM lifetime means more voids, and vice versa. It is shown in Figure that thinner cobalt liner thickness corresponds with shorter EM lifetime, meaning more voids.
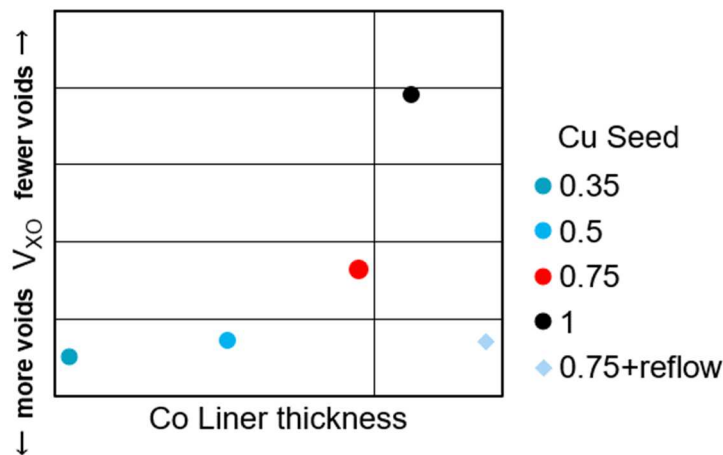

Figure 13: Vxo as a function of Co Liner Thickness. The metric of V_{xo} is plotted against Co liner thickness in terms of wafer average. The circular data points are from no reflow splits, and the diamond data point is from with reflow splits. The circular data points follows nice trend versus Co liner thickness, which agrees with expectation from process point view. The no-reflow data point flies away the trend.

Similar to the results in many previous figures, the diamond data point from reflow split in Figure falls out of the trend shown by the data points from non-reflow splits. With reflow, the microstructure of copper lines can significantly different from those without reflow.

To summarize the results from the metric of V_{xo}, lower values V_{xo} indicates more voids and vice versa. This relationship matches the expectation based on the knowledge of the process. This is the first indicator that V_{xo} is a good metric for voids. The metric of V_{xo} is also evaluated against EM lifetime, which is a known indicator of the amount of voids when all other processes are the same while cobalt

liner thickness varies. The results show that more voids in copper lines corresponding to both lower V_{xo} and shorter EM lifetime. This is the 2nd indicator that V_{xo} is a good metric for void measurement.
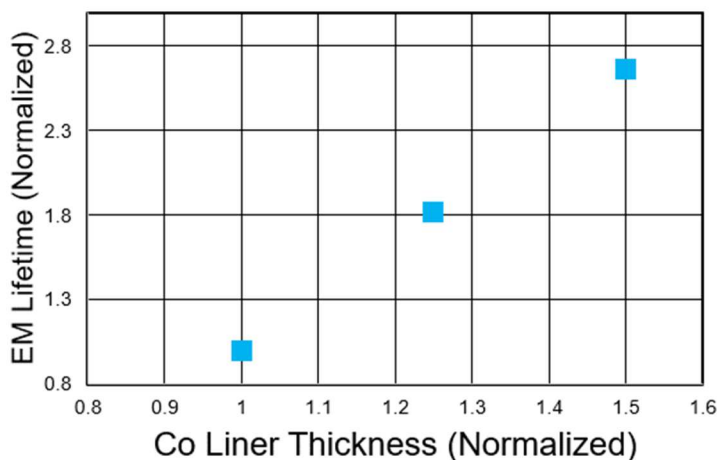

Figure 14: EM Lifetime as a function of Co Liner Thickness. This plot shows the relationship between EM lifetime in y axis and the Co liner thickness in x axis. The EM lifetime is defined here as the time it takes to fail 50% devices. With all parameters same, longer EM lifetime usually indicates fewer voids.

Combining both indicators, it can be concluded that the metric, V_{xo}, is a reliable measurement of voids in copper lines.

3.5 Throughput improvement with the assistance of ML

V_{xo} is validated as a good metric of measuring voids in copper lines, but it involves both XRF and scatterometry measurements. It is known that XRF has lower throughput than scatterometry, and it is always desired in the industry to improve throughput, which reduces cycle time and cost. In this section, we will show that the throughput can be improved with the assistance of machine learning algorithms.

The measured V_{xo} from hybrid metrologies of XRF and scatterometry is used as reference data for machine learning training with respect to the collected scatterometry raw spectra per chip. The well-trained machine learning algorithm is capable of correlating the features of raw spectra with the reference data. Therefore, the developed machine learning algorithm can accurately predict the parameter of V_{xo} based on the collected scatterometry spectra on a different wafer, even when there is no XRF measurement on this wafer. The description of machine learning methods was discussed in section 2.3.

Figure is a plot of the predicted V_{xo} from established machine learning algorithm against the measured V_{xo}. This figure shows that the predicted V_{xo} strongly correlates with the measured V_{xo} with an accuracy of ~ 90%. The linear regression equation with R square is also shown in Figure . To summarize, the throughput for measuring voids using V_{xo} can be as high as scatterometry with the assistance of machine learning, but still with the fidelity of approximately 90%.
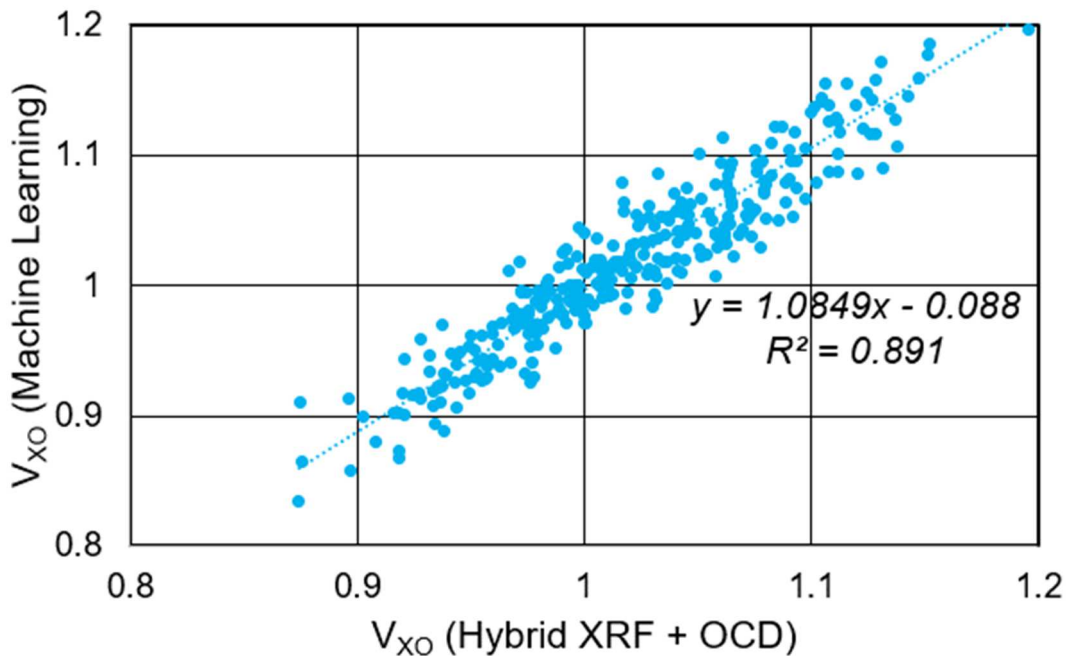
Figure 15: Comparing machine learning and hybrid results. The machine learning method is employed to predict V_{xo} based only on scatterometry raw spectra. The actual measured V_{xo} is used as reference for machine learning algorithm setup with respect to scatterometry raw spectra. The predicted Vox from machine learning highly correlates with the actual measured V_{xo} from hybrid metrologies.

4. CONCLUSIONS

In this work, we demonstrated that the amount of voids in copper lines can be measured inline by employing hybrid metrologies, with a combination of LE-XRF and scatterometry. Two candidate metrics, resistivity and V_{xo}, are investigated as a good measurement of voids in metal lines. Our results show that resistivity is not a reliable measurement of the amount of voids in metal lines. This is because the effect of the cross-sectional area of Cu lines on the resistivity overshadows the contribution of voids to the resistivity.

The metric of V_{xo} measured from hybrid metrologies between LE-XRF and scatterometry is proved to be a good measurement of voids in metal lines. First, the result, that lower V_{xo} indicates more voids, matches the expectation based on the process knowledge. Secondly, the parameter of V_{xo} as a reliable measurement of voids is validated with respect to EM lifetime. Both lower values of V_{xo} and shorter EM lifetime tends to give similar results (more voids). Therefore, the metric of V_{xo}, measured by hybridizing XRF metrology with scatterometry, can be a good measurement of the amount of voids in metal lines.

This work also demonstrated that the throughput of measuring the parameter V_{xo} can be improved as high as scatterometry with the assistance of the machine learning algorithm. It is shown that the

predicted V_{xo} from trained machine learning algorithm matches the actual V_{xo} with a fidelity of 90%, even if there is no XRF measurement involved. This helps to reduce cost in manufacturing.

The experimenting condition with reflow fails out the trend of non-reflow data points due to the possible microstructure difference in Cu lines that the reflow produces. Further investigation is necessary to fully understand the behavior of reflow conditions.

ACKNOWLEDGMENTS

REFERENCES

1. Mechanism and improvements of Cu voids under via bottom, By C-H Lee and R-K Shiue, Solid State Technology, 2018.
2. Ru liner scaling with ALD TaN barrier process for low resistance 7 nm Cu interconnects and beyond, K. Motoyama, et al., Proc. of IEEE IITC, 6.1 (2018)
3. EM enhancement of Cu interconnects with Ru liner for 7 nm node and beyond, K. Motoyama, et al., Proc. of IEEE IITC, 12.3 (2019)
4. PVD Cu Reflow Seed Process Optimization for Defect Reduction in Nanoscale Cu/Low-k Dual Damascene Interconnects Electrochemical/Electroless Deposition, J. Electrochem. Soc. 166, D211-D3215, 2013.
5. Stacked nanosheet gate-all-around transistor to enable scaling beyond FinFET, N. Loubet, T. Hook, et al., 2017 Symposium on VLSI Technology, Kyoto, 2017, pp. T230-T231.
6. Interpreting plasmonic response of epitaxial Ag/Si(100) island ensembles, D. Kong, L. Jiang, and J. Drucker, J. Appl. Phys. 118, 213103 (2015).
7. Tuning Ag/Si(100) island size, shape, and density, D. Kong, J. Drucker, J. Appl. Phys. 114, 144310 (2013).
8. Novel hybrid metrology for process integration of gate all around (GAA) devices, G. R. Muthinti, N. Loubet, et. al., Proc. SPIE 10585, Metrology, Inspection, and Process Control for Microlithography XXXII, 105850Z, 2018.
9. In-line characterization of non-selective SiGe nodule defects with scatterometry enabled by machine learning, D. Kong, R. Chao, et. al., Proc. SPIE 10585, Metrology, Inspection, and Process Control for Microlithography XXXII, 1058510, 2018.
10. Impacts of Liner Metals on Copper resistivity at Beyond 7nm Dimensions, H. Huang et al., 2018 IEEE Int. Interconnect Technol. Conf. /Adv. Met. Conf., pp. 13, 2018.